Paper

A Quantum Chemical Study of the Retinal of Squid Rhodopsin

Yoshinori Nagai*,[1], Masashi Kito[1], Hiroshi Kagawa[2], and Ted Maddess[3]

(Accepted 18 January 2011)

Synopsis: The squid retinal structure obtained from the Protein Data Bank (PDB ids 2Z73 and 2ZIY) is studied in a quantum chemistry method using MOPAC2009 based on a semi-empirical method with PM6 parametrization. The interaction between retinal and light (an electromagnetic field) is effectively described by the interaction between dipoles and electromagnetic fields. Thus we investigated the dipole moment and effective charge distribution of retinal. We also looked at molecular orbitals, especially the HOMO (highest occupied molecular orbital) and LUMO (lowest unoccupied molecular orbital). MO shifting between a double bonded site and single bonded site is seen by comparing HOMO and LUMO results. Retinal changes its conformation from cis to trans at carbon 11. This carbon's effective charge is very small so that it is free from electric interactions. Then it can change conformation with a small change in energy.

1. Introduction

Squids can detect linearly polarized light [1–4], and recognize patterns formed by polarized light [5–8]. This ability of squids is here explained by an interaction between retinal in their rhodopsin and the incoming electromagnetic waves from a microscopic viewpoint, and the global arrangement of rhodopsin pigment molecules from a macroscopic viewpoint [8]. In the present paper, we investigate the microscopic mechanism, that is, photon absorption by rhodopsin even though many studies had been carried out [10–17]. Here the microscopic mechanism is followed via quantum mechanical dynamics [17, 19–20]. The photon absorption occurs at the retinal in every rhodopsin molecule by the interaction between the charge distribution of retinal [18] and the electromagnetic wave [10–17]. This interaction can be effectively described by the dipole moment of retinal and the polarized vector field of the electromagnetic field [10]. We therefore investigate the effective charge distribution and dipole moment of a squid retinal molecule as a first step for the understanding of the recognition mechanism for polarized light in the squid visual system. It is usually said that, photon absorption is the trigger for a cis-to-trans conformation change in the retinal [18–20]. Thus the changes of effective charge distribution and dipole moment of the retinal are investigated in a quantum chemical manner PM6 [24]. The actual calculation is performed on the computer software MOPAC2009 [23].

The structure of squid retinal can be found in the Protein Data Bank (PDB). There are two kinds of X-ray crystallography structure data, namely, 2Z73 [21] and 2ZIY [22] as defined by their PDB identification numbers. These two are different from each other in two ways. One is the X-ray

---

* Corresponding author

[1] Center for Information Science, Kokushikan University

[2] Physics Laboratory, Nippon Medical School

[3] Research School of Biology, Center for Visual Sciences, and ARC Centre of Excellence in Vision Science, Australian National University

diffraction resolution, that is, 0.25 nm for 2Z73, and 0.37 nm for 2ZIY. The other point is that 2Z73 has two polymer chains A, B, and 2ZIY has one polymer chain A. As for ligands, 2Z73 includes six, while 2ZIY two. Both include the ligand retinal so we therefore use both PDB data sets.

In the next section, we briefly describe squid retinal, and the software used to calculate the effective charge of each atom in squid retinal, and the dipole moment, namely, the MOPAC2009 [23], and PM6 methods [24]. The results for charge distribution and dipole moment are shown in section 3. We compare these quantities for the cis and trans conformations. Charge distribution slightly changes between the cis and trans conformations. We discuss the meaning of those small changes in section 5. The molecular orbitals, HOMO and LUMO, are shown in section 4. A small difference between 2Z73 and 2ZIY is seen, and also see a difference between their cis and trans conformations.

2. Material and Method

We downloaded the data files 2Z73 and 2ZIY from the RCSB Protein Data Bank (www.rcsb.org), and cut out the retinal ligand part from PDB data (HETATM 5646 to 5665 for 2Z73, and HETATM 2928 to 2947 for 2ZIY). The X-ray crystallography data of retinal has 20 carbons only. Thus we added hydrogen atoms and an oxygen atom (see Fig. 1), and then the locations of those added atoms were determined at the energy minimized sites. After these treatments, we submitted these data to MOPAC2009 [23]. MOPAC 2009 is a semi-empirical method of quantum chemical calculations. It uses the PM6 method, which produces a more complete parameter optimization for the allowed 70 elements [24].

The retinal found in the PDB data, 2Z73 and 2ZIY, is in the 11-cis conformation. The most different feature of the two structures are the 6-member ring and carbon zig-zag line components. The trans conformation was obtained by 180 degree rotation around the C_{10} to C_{11} bonding line. The trans-form of the two retinal structures were input into MOPAC2009. The MOPAC2009 output provides the effective charge of each atom, dipole moment, and molecular orbital (MOs). The carbon numbering and cis and trans conformations are shown in Fig. 1. Usually the C_1 to C_{15} carbons are considered in the structure of retinal, so we examined the results for those 15 carbons only.

3. Effective Charge Distribution and Dipole Moment of Squid Retinal

To aid understanding of results obtained from MOPAC2009, we depicted the effective charge of each atom and the dipole moment for 4 cases: cis and trans conformations of 2Z73, and those of 2ZIY. As seen from Fig. 2 and Fig. 3, almost zero effective charge exists on carbon 11 (C_{11}). The effective charge change of each atom was obtained from the procedure, that is, effective charge of cis conformation minus that of the trans conformation. Thus, positive changes correspond to increases of positive charge, and decreases to negative charges. This case is shown in Fig. 4. Increases or decreases of charge, whether negative or positive, are shown in Fig. 5. In Fig. 5, decreases of effective charge from cist to trans conformations independent of sign are depicted in upper panel, and increases in the lower panel. The main change of effective charge was a decrease on the confor-

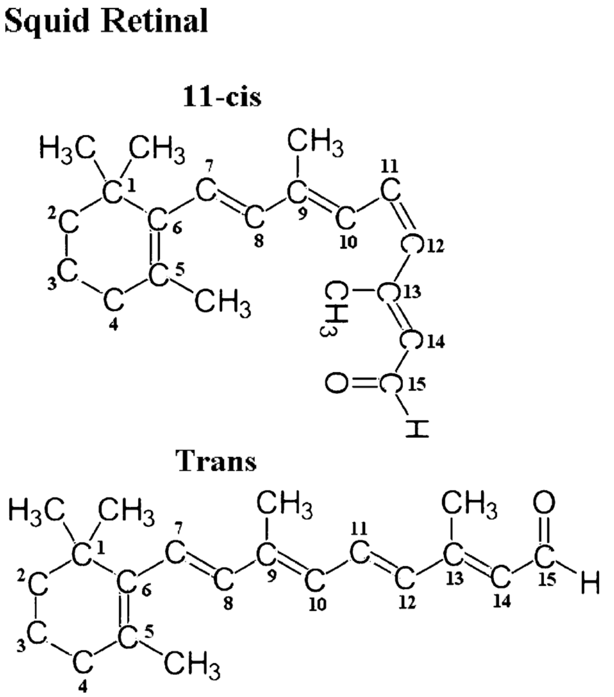

Fig. 1 Cis and trans conformations of retinal and the carbon numbering scheme

mation change from the cis to trans conformation. The maximum change of effective charge occurred at C_{10} The upward direction is decreasing, and downward direction increasing.

At C_{11} the effective charge decreased in 2ZIY, but increased in 2Z73. Opposite changes of effective charge also occurred at C_4, C_5, and C_6. Both PDB data give maximum decreases of effective charge at C_{10}. Overall, effective charge changes appeared on the conformation side of cis-to-trans structure changes.

Calculation results of dipole moments using MOPAC2009 are given in Table 1. Table 1 shows that the dipole moment of retinal decreases its size with the conformation change from cis to trans. The magnitudes of the decreases for the cis to trans conformation change were 0.266 D for 2Z73, and 0.329 D for 2ZIY. The magnitude differences between 2Z73 and 2ZIY were decreases of 0.493 D in the cis conformation, and 0.556 D in the trans conformation. From these changes of dipole moment, we know that a small decrease of dipole moment magnitude occurs for the cis to trans conformation change in retinal. Decreases of dipole moments can be interpreted as an energy transfer from the electromagnetic field to the amino acids of rhodopsin interacted with the retinal. The dipole moments of the cis conformation for 2Z73 and 2ZIY are depicted in Fig. 6. The origin of the dipole moment vector is the averaged center of the charge distribution of the electron orbitals. As seen from Fig. 6 the starting point of the dipole moment vector exists near the hydrogen atom bound to C_{10}.

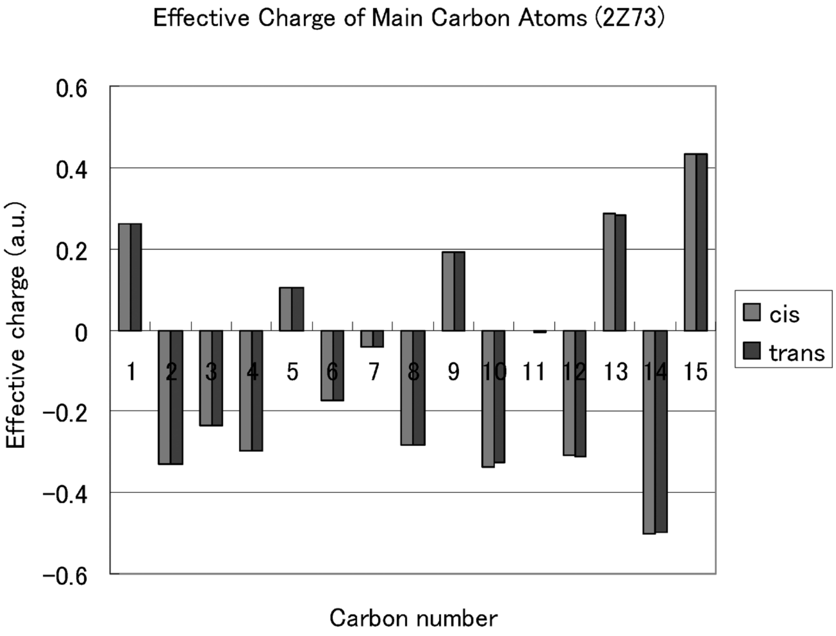

Fig. 2 Effective charge distribution of 2Z73.

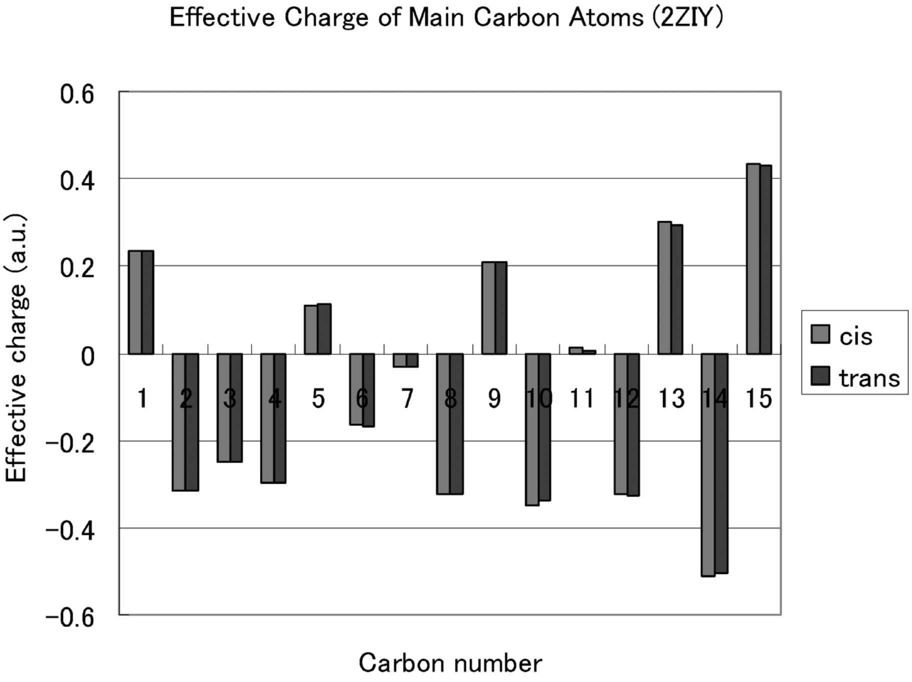

Fig. 3 Effective charge distribution of 2ZIY.

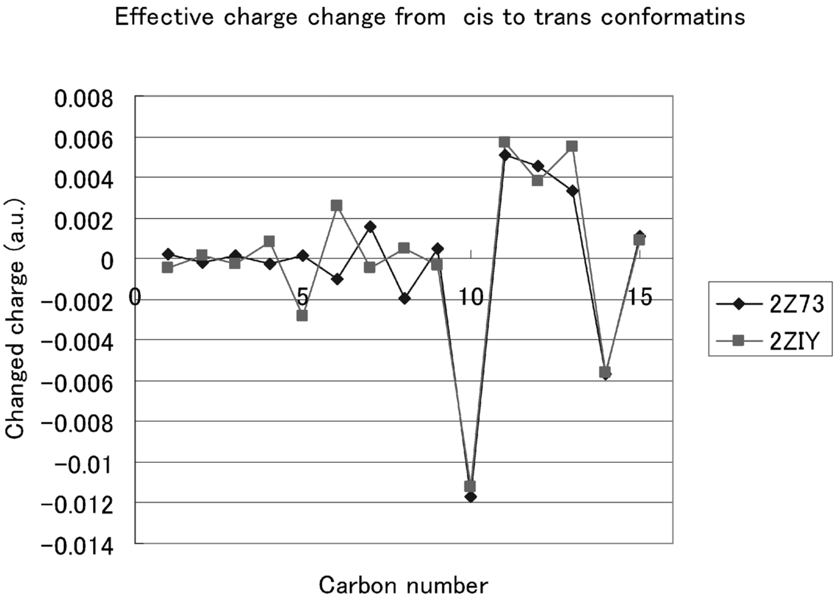

Fig. 4 Change of effective charge caused by the cis to trans conformation change

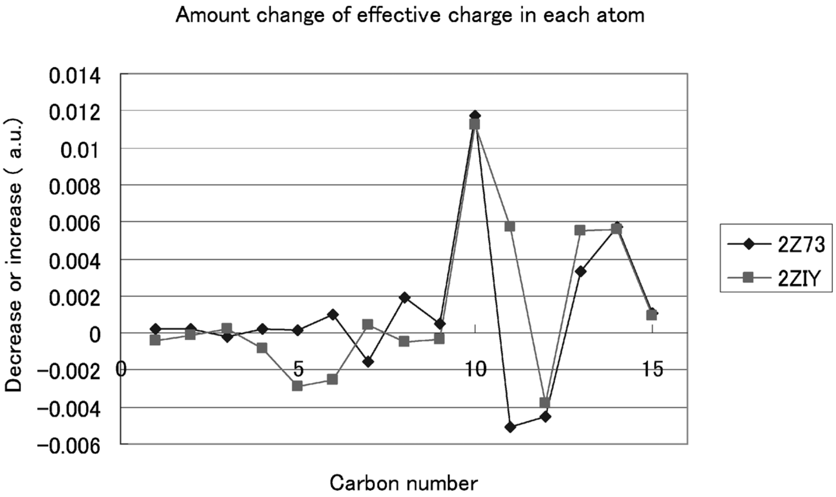

Fig. 5 Decreases and increases of effective charge.

Table 1 Dipole moments of cis and trans conformations in 2Z73 and 2ZIY (Debye unit)

	2Z73	2ZIY
Cis	8.058 D	7.565 D
Trans	7.792 D	7.236 D

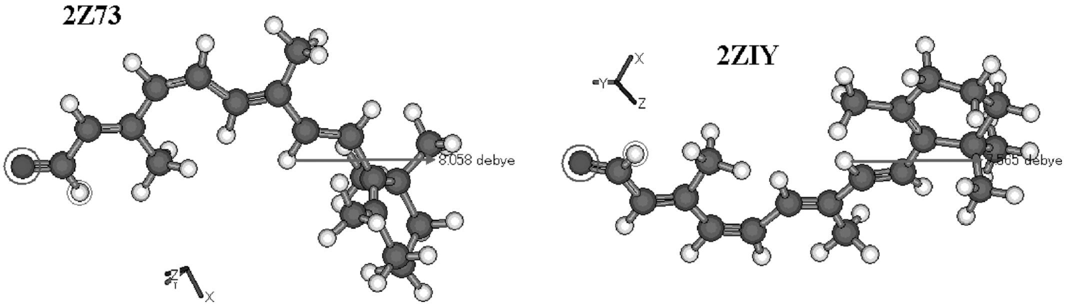

Fig. 6 Dipole moment of the cis conformation in 2Z73 and 2zIY.

4. Highest Occupied Molecular Orbital and Lowest Unoccupied Molecular Orbital

MOPAC2009 is software for quantum chemical calculations that principally solves the Schrödinger equation for chemical compounds. This means that state vector ψ_j for the energy state E_j is obtained as the canonical state of the electrons. Usually electron transitions occur from the highest occupied eigen state to another unoccupied state depending on the interaction energy. We therefore examined the rhodopsin state vectors corresponding to the highest and lowest unoccupied state. In quantum chemistry terminology, these are called HOMO (highest occupied molecular orbital) and LUMO (lowest unoccupied molecular orbital).

In this section, we show the HOMO and LUMO results for cis and trans conformation structures of 2Z73 and 2ZIY. Figs 7 and 8 respectively show HOMO data for 2Z73 and 2ZIY, while Figs 9 and 10 show the corresponding LUMO data. Figs 11–14 show HOMO and LUMO data for the trans conformation of these PDB data. The apparent molecular orbitals (MO) are essentially analogous to each other on each site. The differences between 2Z73 and 2ZIY in the molecular orbitals are that the MO around the oxygen site of 2ZIY is smaller than that of 2Z73, whereas the MO of the 6-member ring of 2ZIY is bigger than that of 2Z73. The Methyl group in 2ZIY becomes especially active in the HOMO state. In 2Z73, however, there is little evidence of an orbital in that area. Figs 7–14 also indicate that the molecular orbital shifts from the double bonded site to a single bonded site on the conformation change from cis to trans.

The electrons in the HOMO states are easier to transit to another state than the electrons of the lower energy state. The HOMO state is widely distributed across the rhodopsin molecule. This means that the reaction response to any interaction occurs along the carbon chain. The LUMO state of rhodopsin reacts at the same area as the HOMO state. Thus photon absorption occurs at this area as suggested by the literature [18–20].

5. Summary and Discussion

The electron distribution gives the effective charge of each atom. We summarize the sign of the effective charge at each atom in Fig. 15. There is an electron orbital shift from double a bonded site to a single bonded site according to the cis to trans conformation state, which relates to the effective

Fig. 7 HOMO of original PDB data conformation of 2Z73

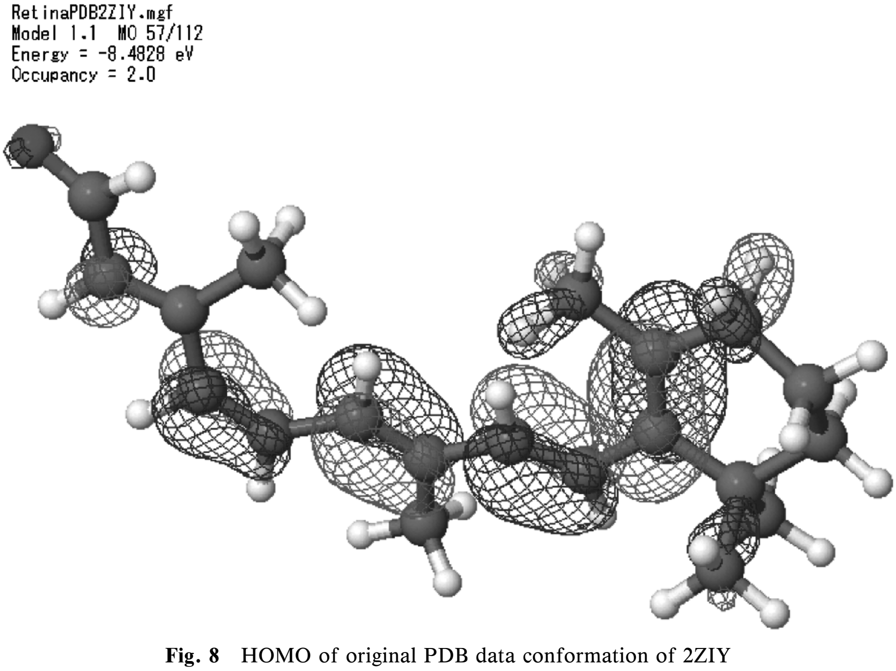

Fig. 8 HOMO of original PDB data conformation of 2ZIY

charge of C_7, C_9, C_{11}, C_{13}, and C_{15}. As seen from the summary figure of the effective charge sign (Fig. 15), the effective charges of C_9, C_{13}, and C_{15} are positive. By contrast C_{11} is almost zero. The effective charge of C_7 is a small negative value. Thus we can understand the orbital shift between

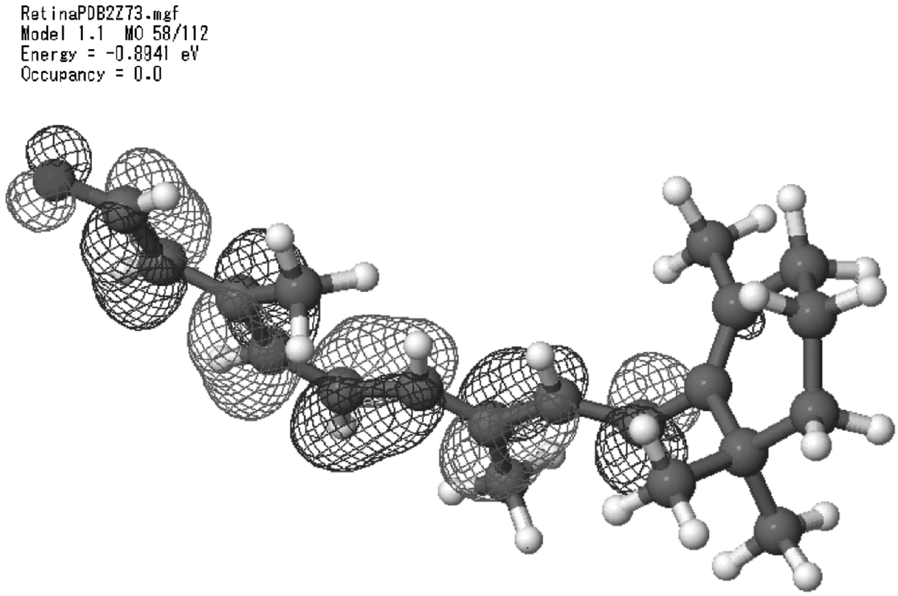

```
RetinaPDB2Z73.mgf
Model 1.1  MO 58/112
Energy = -0.8941 eV
Occupancy = 0.0
```

Fig. 9 LUMO of original PDB data conformation of 2Z73

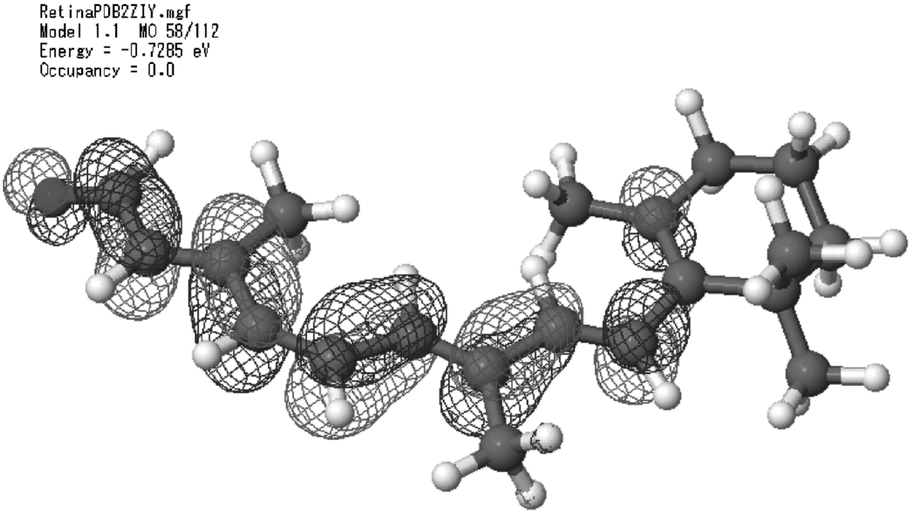

```
RetinaPDB2ZIY.mgf
Model 1.1  MO 58/112
Energy = -0.7285 eV
Occupancy = 0.0
```

Fig. 10 LUMO of original PDB data conformation of 2ZIY

the double and single bonded sites as just a shift between double bonding and single bonding. We also know from Fig. 15 that the positive sign of effective charge appears at carbons having three or four bonds to other carbons or oxygen (e.g. C_1, C_{15}).

Photon absorption occurs between the dipole of retinal and the electromagnetic field [10]. Following article 10, the total photon absorption rate is following (eqs 5.36 and 5.38 of ref. 10),

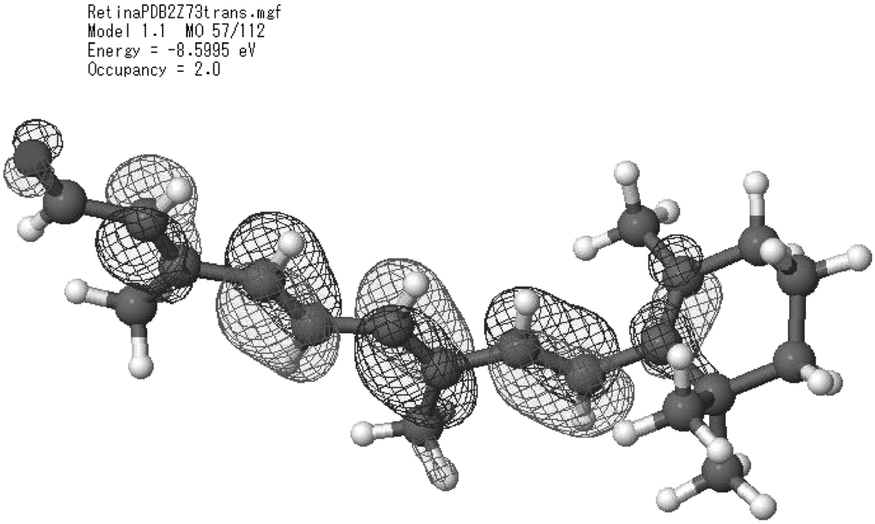

Fig. 11 HOMO of trans conformation of 2Z73

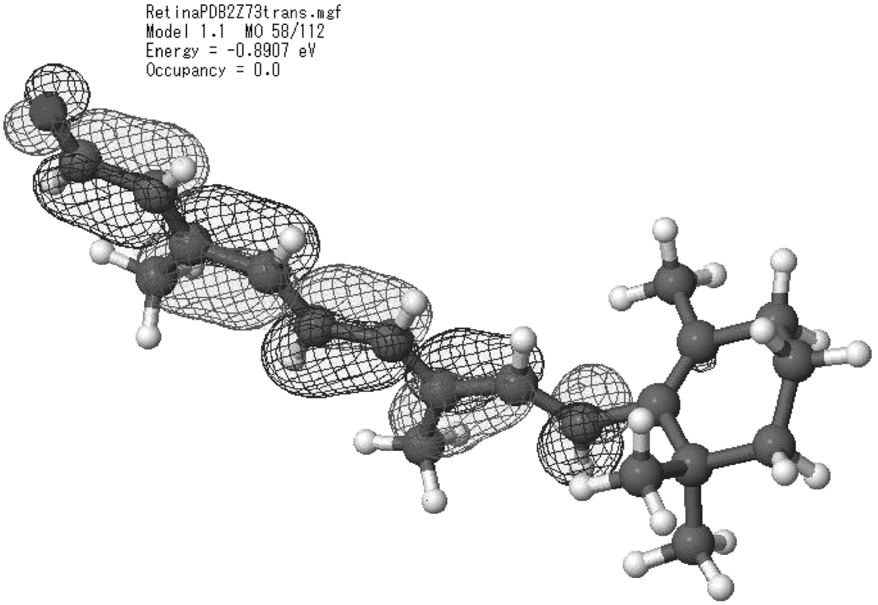

Fig. 12 LUMO of trans conformation of 2Z73

$$w_{abs}(m \rightarrow k) = \frac{2\pi}{\hbar} \left| U_{km}(\vec{k}) \right|^2 \rho(E_m + \hbar_\omega) \tag{1}$$

With

$$U_{km}(\vec{k}) = -\frac{eA_0}{2mc} < k \left| e^{i\vec{k}\cdot\vec{r}}\, \vec{\varepsilon} \cdot \vec{p} \right| m > \tag{2}$$

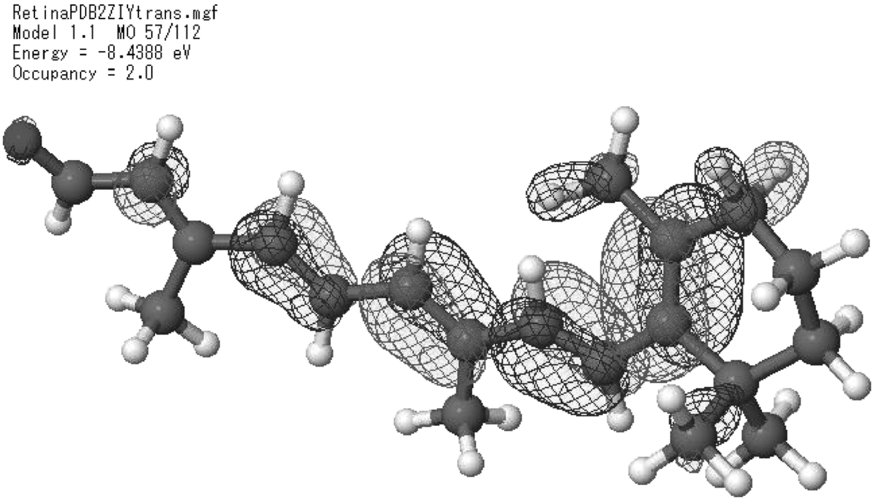

Fig. 13 HOMO of trans conformation of 2ZIY

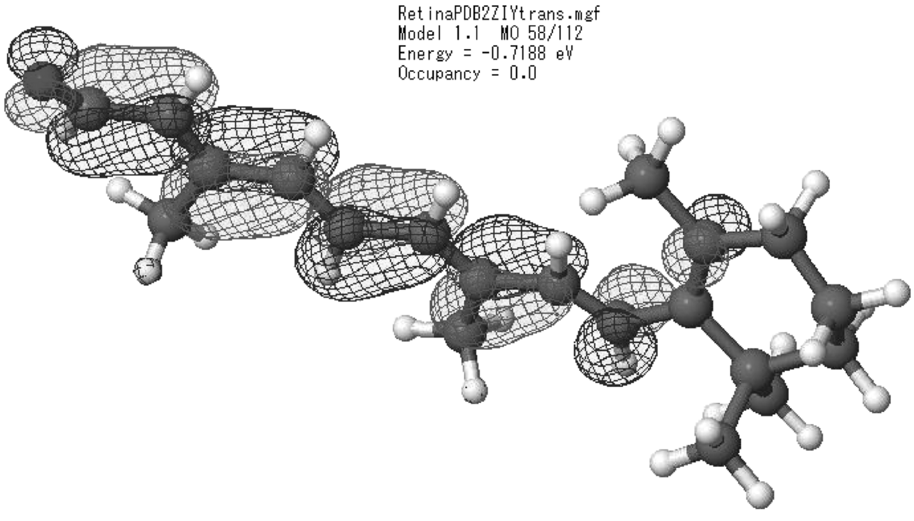

Fig. 14 LUMO of trans conformation of 2ZIY

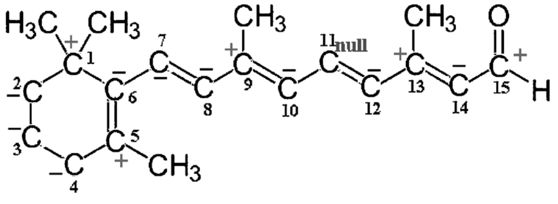

Fig. 15 Effective charge distribution of squid retinal. The symbols +, −, and null indicate effective charges that are positive, negative, and very small respectively.

A_0 is amplitude of vector potential of the electromagnetic field that relates to number of photons per unit volume [10], namely, the energy density of the field, and $\bar{p}$ is the momentum vector of an electron. If the wavelength of the electromagnetic field is in the visible light range, the approximationis $e^{i\bar{k}\cdot\bar{r}} \approx 1$ is valid. Thus this approximation yields following results (5.39 of ref.10),

$$U_{km}(\bar{k}) = -\frac{eA_0}{2mc} < k \left| \bar{\varepsilon} \cdot \bar{p} \right| m > . \tag{3}$$

The momentum vector and position vectors satisfy the following relation through the Hamiltonian,

$$\bar{p} = \frac{im}{\hbar} [H, \bar{r}]. \tag{4}$$

The equation (4) implies the momentum can replace the position so that the dipole moment approximation becomes valid for the visible light region around there. Following [10] eq. (2) has the approximation as follows,

$$U_{km}(\bar{k}) = \frac{\mp iA_0\omega}{2c} \bar{\varepsilon} \cdot \bar{\mu}_{km}, \tag{5}$$

where $\bar{\mu}_{km}$ is the dipole moment defined as,

$$\bar{\mu}_{km} = e < k \left| \sum_i \bar{r}_i \right| m > . \tag{6}$$

The above eqs (5) and (6) are eqs 5.43 and 5.42b of ref.10. Notice that $\bar{\varepsilon}$ is the polarization vector of the electromagnetic field using vector potential $\bar{A}$. We therefore considered vision of polarized light in squids using the above equations as the interaction between the polarization direction of electromagnetic field and dipole moment of retinal in a rhodopsin. This means that to provide a dichroic detector the rhodopsin molecules, and so too the retinal, must be oriented within the photoreceptor membrane. That may be aided by a tetramer structure of squid rhodopsins that aligns the dipoles of 4 retinals [21].

References

[1] R. Hubbard, R. C. C. ST. George, The rhodopsin system of squid, *J. Gen. Phisiology* **41** (1958) 501–528.

[2] T. W. Cronin, N. Shashar, R. L. Caldwell, J. Marshall, A. G. Cheroske, T. H. Chiou, Polarization vision and its role in biological signaling, *Integr. Comp. Biol.* **43** (2003) 549–558.

[3] N. Shashar, P. S. Rutledge, T. W. Cronin, Polarization vision in cuttlefish- a concealed communication channel?, *J. Exper. Biol.*, **199**, (1996) 2077–2084.

[4] T. H. Chiou, L. M. Maethger, R. T. Hanlon, T. Cronin, Spectral and spatial properties of polarized light reflections from the arms of squid (***Loligo pealeii***) and cuttlefish (***Sepia officinalis L.***), J. Exp. Biol. 210 (2007)3624–3635.

[5] A. J. Shohet, R. J. Baddeley, J. C. Anderson, E. J. Kelman, D. Osorio, Cuttlefish responses to visual orientation of substrates, water flow and a model of motion camouflage, *J. Exper. Biol*, **209** (2006) 4717–4723.

[6] E. J. Kelman, R. J. Baddeley, A. J. Shohet, D. Osorio, Perception of visual texture and the expression of disruptive camouflage by cuttlefish, ***Sepia officinalis***, Proc. R. Soc. **B274** (2007) 1369–1375.

[7] E. J. Kelman, D. Osorio, R. Baddeley, A review of cuttlefish camouflage and object recognition and evidence for depth perception, *J. Exper. Biol.*, **211** (2008) 1757–1763.

[8] S. Zylinski, D. Osorio, A. J. Shohet, Perception of edges and visual texture in the camouflage of the common cuttlefish, ***Sepia officinalis***, *Phil. Trans. R. Soc.*, **B364** (2009) 439–448.

[9] T. Hara, R. Hara, Distribution of rhodopsin and retinochrome in the squid retina, *J. Gen. Physiology*, **67** (1976) 791–

805.
[10] G. C. Schatz and M. A. Ratner, *Quantum Mechanics in Chemistry*, Chapter 5 Interaction of Radiation with Matter, pp. 78–110 Dover, 2002.
[11] T. Shieh, M. Han, T. P. Saknar, S.O. Smith, The steric trigger in rhodopsin activation, J. Mo. Biol. 269 (1997) 373–384.
[12] R. R. Birge, Photophysics and molecular electronic applications of the rhodopsin, Annu. Rev. Phys. Chem. 41 (1990) 683–733.
[13] H. Kandori, H. Sasabe, K. Nakanishi, T. Yoshizawa, T. Mizukami, Y. Shichida, Real-time detection of 60-fs isomerization in a rhodopsin analog containg eight-membered-ring retinal, J. Am. Chem. Soc., 118 (1996) 1002–1005.
[14] D. Fotiadis, Y. Liang, S. Filipek, D. A. Saperstein, A. Engel, K. Palczewski, The G protein-coupled receptor rhodopsin in the native membrane, FEBS Letters 564 (2004) 281–288.
[15] G. FX Schertler, Structure of rhodopsin and the metarhodopsin I photointermediate, Cur. Opi. Struc. Biol., 15 (2005) 408–415.
[16] D. Mustafi, K. Palczewski, Topology of class a G protein-coupled receptors: Insights grained from crystal structure of rhodopsins, adrenergic and adenosine receptors, Mol. Pharmacology, 75 (2009) 1–12.
[17] A. Bifone, H. J. M. de Groot, F. Buda, Ab initio molecular dynamics of rhodopsin, Pure & Appl. Chem 69 (1997) 2105–2110.
[18] D. C. Petersen, R. A. Cone, The electric dipole moment of Rhodopsin solubilized in Triton X-100., Biophyscal J. 15 (1975) 1181–1200.
[19] M. V. Altaisky, V. N. Gorbachev, F. Pichierri, Coherent signal amplification in rhodopsin media, Пмсьма в ЭЧАЯ T.4 (2007) C. 260–266.
[20] N. S. Vassilieva-Vashakmadze, R. A. Gakhokdze, A. R. Gakhokidze, Mechanism of photoisomerization of the rhodopsin chromophore, Biochemistry (Moscow) 73 (2008) 730–732.
[21] M. Murakami and T. Kouyama, Crystal structure of squid rhodopsin, *Nature*, **453** (2008) 363–367.
[22] T. Shimamura et al., Crystal structure of squid rhodopsin with intracellular extended cytoplasmic region, *J. Biol. Chem.*, **283** (2008) 17753–17756.
[23] MOPAC2009 J. J. P. Stewart http://openmopac.net/
[24] J. J. P. Stewart, Optimization of parameters for semiempirical method V: Modification of NDDO approximations and application to 70 elements, J. Mol. Model 13 (2007) 1173–1213.